DESIGN AND DEVELOPMENT OF THE MAIN PARACHUTE FOR THE BEAGLE 2 MARS LANDER

Edward J. Fallon II and Robert Sinclair
Irvin Aerospace Inc
Santa Ana, California

Abstract

This paper addresses the successfully completed design and development efforts of the Beagle 2 main parachute conducted over its entire course of *less than three (3) months!* In general, the following topics are presented: System & Parachute Aerodynamics, Main Parachute Design, and Verification Testing of Parachute Performance.

Introduction

Mars Express is the first flexible mission of the ESA Horizons 2000 Scientific Program and will be launched in May / June 2003. The mission is dedicated to the orbital and possibly in-situ study of the interior, surface and atmosphere of the planet Mars.

As a part of the Mars Express mission, the Beagle 2 lander will study at its landing site in Isidis Planitia, the morphology and geology, the chemical and mineralogical composition of Martian surface rocks and soils, and other physical properties of the surface materials. One of the main objectives of the Beagle 2 mission is exobiology (i.e. signatures of life).

The Beagle 2 lander is designed to address these requirements with meteorology, stereo imaging and organic chemistry packages and a robotic arm incorporating spectroscopy, imaging and a sampling mole to return samples to the lander.

The Beagle 2 lander will descend to the Martian surface using a Mars Pathfinder-like sequence comprising of an aeroshell, two parachute stages and an airbag landing system.

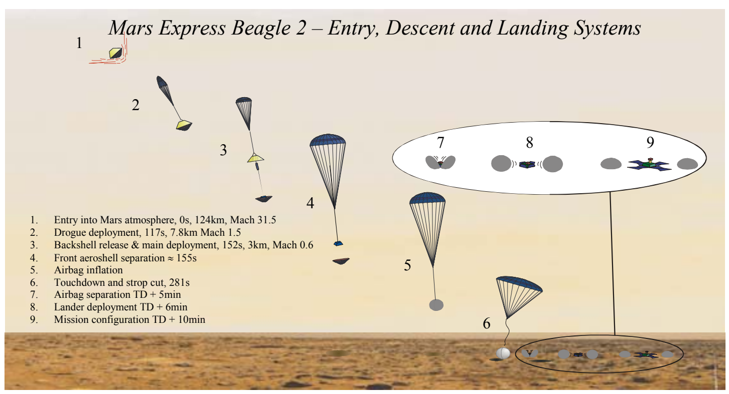

Figure 1

Operational Sequence

The Beagle 2 spacecraft enters the Martian atmosphere decelerating under the influence of the front aeroshell. At approximately Mach 1.5, a mortar fires, deploying the drogue parachute. The drogue fully inflates, and further decelerates the spacecraft from Mach 1.5 to a range of Mach 0.4 to 0.6. At this speed, the aeroshell release mechanism activates to sever the attachment holding the front and rear halves of the aeroshell in place. The drag of the drogue pulls the rear half of the aeroshell away from the spacecraft. The main parachute, which is attached and stowed inside the internal structure of the rear aeroshell, then deploys. On inflation, the main parachute decelerates the spacecraft to a terminal velocity of 16 to 18 m/s over a period of approximately 15 seconds. During the deployment / inflation process of the main parachute, the front aeroshell separates from the Beagle 2 lander.

At a height of approximately 200 m above the Martian surface, the airbags inflate. At lander touchdown, the PRM activates, severing the main parachute strop, that in turn releases the main parachute from the lander. The airbags attenuate the lander's kinetic energy as a result of touchdown. After airbag attenuation, the airbags separate from the lander and the lander deploys to its final mission configuration.

Figure 1 provides a summary depiction of the Beagle 2 entry, descent, and landing operational sequence.

Establishing Design & Performance Criteria

Performance Requirements

The relevant main parachute operational performance requirements are summarized in Table 1.

Table 1. System Performance Requirements

Condition	Flight Operation
Atmospheric Density (Loads)	0.01220 to 0.01460 kg/m^3
Atmospheric Density (Terminal Descent)	0.0188 kg/m^3
Flight Path Angle (from Horizontal)	-43° to - 63°
Deployment Velocity	95 to 146 m/s
Temperature	230°K to 300°K
Gravity	3.72 m/s^2
Payload Mass	49.6 kg
Payload Drag Area	0.7 m^2
Inflation Load	≤ 5.88 kN
Rate of Descent	≤ 18 m/s 16 m/s (target)
Parachute Assy Mass	≤ 3.237 kg (excluding PRM)
Parachute Volume	~ 0.008342 m^3
Parachute System Length	≥ 40 m

System Aerodynamics

An aerodynamic decelerator system generally consists of multiple aerodynamic bodies coupled together by some form of elastic restraint. Typically, this system consists of a suspended payload (e.g., spacecraft, missile, aircraft, etc.) tethered to one or more parachutes. The interactions between these multiple aerodynamic bodies form a complex aerodynamic flow pattern, which, in turn, establishes the aerodynamic performance of the overall system. Therefore, in order to properly assess the aerodynamics of the parachute in a decelerator system, the influence of the *suspended payload aerodynamics* on the parachute must first be understood to establish the parachute aerodynamic performance and thus, the overall aerodynamic performance of the decelerator system.

Forebody Wake Effects

An aerodynamic decelerator system, consisting of a suspended payload (or rather forebody) with a parachute in tow, establishes a highly complex, non-linear aerodynamic flow inter-relationship between the forebody and the parachute. As the parachute is in tow, it is frequently influenced by the *disturbed flow* created by the forebody. This interaction of the disturbance of the flow field by the forebody and its influence on the aerodynamic performance of the parachute is commonly referred to as *forebody wake effects*. Forebody wake effects are generally a function of [1]:

- Shape of the forebody
- Forebody angle of attack
- Relative space positioning of the forebody to the parachute
- Ratio of the forebody area to the parachute area
- Mach number

Given the highly complex, non-linear nature of the decelerator system flow field, forebody wake effects are often measured by extensive wind tunnel tests. For example, the *Viking, Galileo,* and *Huygens* programs employed extensive wind tunnel tests to determine the influence of the forebody wake effects on the towed parachute[ii,iii,iv]. These wind tunnel tests proved invaluable in establishing the parachute design in meeting the stringent aerodynamic requirements of each respective mission.

For *Viking*, a relative distance between the forebody and parachute of

$$x/d = 9.0$$

where,

x = The distance from the maximum forebody reference diameter to the parachute canopy skirt

d = The maximum forebody reference diameter

yielded a subsonic parachute drag coefficient, C_{D0}, nearly equal to parachute alone values (i.e., no forebody present). For Beagle 2, given that the relative distance between the forebody and parachute is much greater than 9.0 (i.e., x/d ≈ 44) and that the ratio of the forebody area to the parachute area is less compared to *Viking*, forebody wake effects are estimated to have negligible affect on the Beagle 2 main parachute aerodynamic performance.

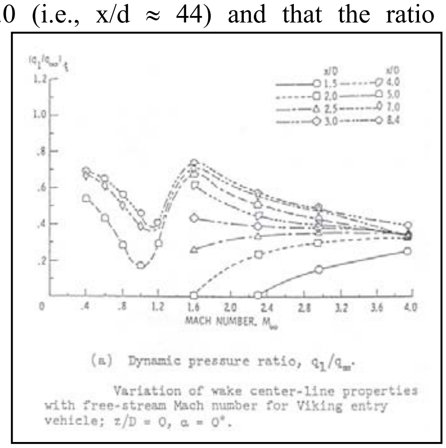

Figure 2

Figure 2 provides wind tunnel test results of forebody wake effects as derived from the *Viking* program[v].

Aeroelasticity

Preisser and Greene[vi] simplified the study of aeroelasticity by modeling the decelerator system as a simple model consisting of two point masses connected by a spring as shown in Figure 3.

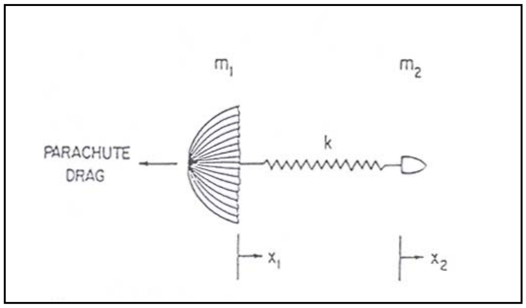

Figure 3

The equations of motion shown for the system in Figure 3 may be written as:

$$m_1 \ddot{x}_1 = \frac{-\rho\, \dot{x}_1^2 C_D S}{2} + k(x_2 - x_1) \qquad \text{Eqt.(1)}$$

$$m_2 \ddot{x}_2 = -k(x_2 - x_1) \qquad \text{Eqt.(2)}$$

The simple system described by equations (1) and (2) assumes the following:

- Gravity is neglected as it acts uniformly on the system
- The payload (i.e. forebody) drag is negligible compared to the parachute drag
- Internal viscous damping is ignored
- The dynamic pressure is constant throughout inflation (i.e., the decelerator system is an *infinite mass* system*)

Equations (1) and (2) can be combined to form:

$$\ddot{\xi} + \omega^2 \xi = (q_s C_D S_0 / m_1) f(t/t_F) \qquad \text{Eqt. (3)}$$

where,

$f(t/t_F) = C_D S / C_{D0} S_0$ = Non-dimensionalized drag area

$q_s = \rho[\dot{x}_1(0)]^2/2$ = Dynamic pressure at start of inflation

$\omega = (k/m_2 + k/m_1)^{1/2}$ = Natural frequency of system

$\xi = (x_2 - x_1)$

To approximate the range of typically encountered inflation histories, Preisser and Greene set:

$$f(t/t_F) = (t/t_F)^n \quad \text{for} \quad t \le t_F$$

and

$$f(t/t_F) = 1 \quad \text{for} \quad t > t_F$$

Furthermore, to isolate the inflation process from other dynamic effects, Preisser and Greene chose initial conditions such that there was no relative extension, $\xi(0) = 0$, and no relative velocity, $\dot{\xi}(0) = 0$, at the beginning of the inflation event. Duhamel's integral[vii] provides the solution to equation (3).

Figure 4 shows plots of the load amplification factor, M, versus the ratio of the filling time to the natural system period (i.e., t_F / T) where n varies from 1 to 4 and

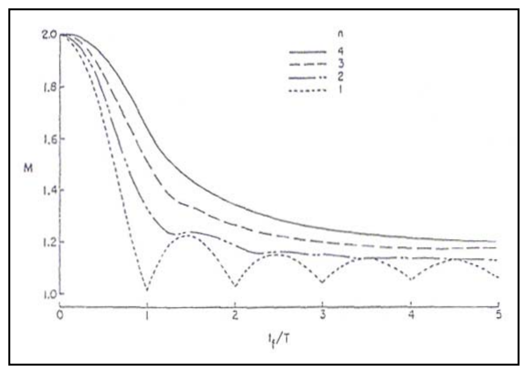

Figure 4

$$M = (m_2 \ddot{x}_2 / q_s C_D S_0)_{max}$$

$$T = 2\pi/\omega$$

From Figure 4, two significant parameters strongly influence the maximum opening loads, or rather dynamic response, of the decelerator system. First, a decreasing parachute inflation time, t_F, increases the maximum opening load. Secondly, an increasing system period, T, (i.e., a decreasing "spring" constant, k, and an increasing parachute mass, m_2) increases the maximum opening load. If one measures the maximum opening load against the product of the maximum drag area and dynamic pressure (both parameters conditioned at the event of canopy full open), then the ratio of these two measures, commonly referred to as

*Note: An *infinite mass* decelerator system is one wherein the system deceleration is considered negligible throughout the entire canopy inflation process until fully open. Thus, the system behaves as though the drag force has no effect on the system mass throughout canopy inflation, hence “infinite mass”.

opening load factor, is directly a function of the aeroelastic properties of the decelerator system.

Another interesting result of the simple model presented by Preisser and Greene is the character of the load history immediately following full parachute inflation. Here the assumption of $\dot{x}_1$ (or $\dot{x}_2$) being nearly constant cannot be made as the system is decelerating rapidly due to the drag force of the parachute. Instead, it is now assumed that the drag area of the parachute remains constant.

By setting,

$$\dot{x}_2/\dot{x}_1 = (1+\phi)$$

where

$$\phi << 1 = \text{Non-dimensional parameter}$$

Equations (1) and (2) can be combined to form:

$$\ddot{\xi} - \left(C_{D0} S_0 \rho \dot{\xi} / 2 m_1 \phi^2\right)\dot{\xi} + \omega^2 \xi = 0 \qquad \text{Eqt. (4)}$$

Equation (4) represents cyclic oscillatory motion of the parachute/payload system about a steady drag loading history wherein the second term of equation (4) represents non-linear damping included in the motion of this system—the amplitude of oscillation of this simple system being dependent upon the *damping* term. As such, equation (4) shows that for a given decelerator system that the amount of *damping* decreases as the atmospheric density decreases. Hence, oscillating load histories initiated by the inflation process should persist in low-density atmospheres (i.e., Mars) even after the parachute drag area becomes steady. Further, should the parachute drag area vary after full inflation (i.e., canopy over-inflation), the oscillatory load history is additionally exacerbated.

In summary, the following general conclusions can be drawn due to system aeroelasticity:

1. For near *infinite mass* decelerator systems (i.e., *Viking*, *Beagle 2*, etc.), increased suspension system elasticity (i.e., a low spring constant, k) and/or increased parachute mass will result in an increase of the parachute opening load. Conversely, decreased suspension system elasticity (i.e., a high spring constant, k) and/or decreased parachute mass will decrease the parachute opening load.

2. Again, for near infinite mass decelerator systems, reducing the canopy inflation time, t_F, increases the parachute opening load. Conversely, increasing the inflation time reduces the parachute opening load.

For parachute deployments in low density atmospheres (i.e., Mars), oscillating load histories initiated by the inflation process will persist as a result of reduced *damping* as opposed to parachute deployments in high density atmospheres (i.e., Earth lower atmosphere) where such oscillatory behavior is almost non-existent (for constant parachute drag area).

<u>Snatch Force</u>

Related to system aeroelasticity, parachute *snatch force* is highly dependent on the decelerator system aeroelastic characteristics. Parachute snatch force is the impact load generated by the impulsive re-acceleration of all or part of the parachute mass at parachute line stretch during deployment. A simplified snatch force equation[viii], is as follows:

$$F_s = \Delta V_{\max}\left(\frac{k m_1 m_2}{m_1 + m_2}\right)^{1/2} \qquad \text{Eqt. (5)}$$

where,

$\Delta V_{\max}$ = The difference in velocities between the parachute and payload at the event of parachute line stretch

From equation (3),

$$\omega = \left(k/m_1 + k/m_2\right)^{1/2} = \left(\frac{k(m_1 + m_2)}{m_1 m_2}\right)^{1/2}$$

Thus, equation (5) may be re-written as:

$$F_s = \Delta V_{\max}\,\frac{k}{\omega} \qquad \text{Eqt. (6)}$$

From equations (5) and (6), the following conclusions can be surmised:

1. Increased system elasticity (i.e., a low spring constant, k) and/or decreased parachute mass will reduce snatch force.

2. Decreased system elasticity (i.e., a high spring constant, k) and/or increased parachute mass will increase snatch force.

3. An increase / decrease in the difference in velocities between the parachute and payload at the event of parachute line stretch will increase / decrease snatch force.

In summary, the principles of aeroelasticity state that in order to minimize parachute opening loads while also minimizing snatch loads, the parachute mass must be as small as practical. As parachute opening loads are generally greater than snatch loads, then ideally, the system elasticity should be as low as practical (i.e., a high spring constant, k) in order to minimize any opening load amplification.

Parachute Aerodynamics

Knowledge of the aerodynamic and operational characteristics of the main parachute design is prerequisite to the design of a dependable descent system and the prediction of the main parachute performance in the flight operational environment.

In simplistic terms, the aerodynamics of parachutes can be viewed as being governed by the inherent characteristics of the canopy as well as the external aerodynamic influences acting upon the canopy structure. A sampling of these inherent canopy characteristics and aerodynamic influences are:

- Planform shape
- Porous nature of the planform shape (i.e., porosity)
- Canopy Size
- Effective Suspension Length
- Mach Number
- Reynolds Number (at very low values)
- Dynamic Pressure

These characteristics, in turn, are generally highly correlated to the elastic nature of the canopy structure as well as the tension and stress loads superimposed upon the canopy structure during flight. Given that these properties vary with both scale and operational conditions (including the non-linear coupling of these characteristics), the emphasis to the importance of full-scale flight testing and the reliance upon a historical record of full-scale flight performance cannot be understated. As such, the flight performance characteristics presented herein are primarily empirical in nature or derived based upon empirical relationships.

Drag Coefficient

Perhaps the most significant parameter of parachute aerodynamic performance is its ability to produce drag efficiently (i.e., maximum drag produced by a minimum of canopy surface area). The drag efficiency is reflected in the term, C_{D0}, a coefficient of aerodynamic drag force related to the total parachute surface area, S_0. For Ringsail parachutes, S_0, commonly referred to as nominal area, is computed as the surface area generated by the gore planform shape inclusive of vent area and slots, but *exclusive of sail fullness*.

The drag coefficient, C_{D0}, varies within a characteristic range largely based upon the external aerodynamic influences acting upon the canopy's elastic structure, how the canopy structure responds to these influences based upon its geometric and mechanical characteristics, and the corresponding aerodynamic flow field established by the canopy's interaction with these influences. As a result, all of these factors are strongly coupled one to another wherein the drag coefficient, on average, varies with any one given state of quasi-equilibrium for any one combination of these said factors. With this said, a number of specific influences and canopy characteristics, as noted above, uniquely affect the drag coefficient. However, for the sake of brevity, those parameters, which most influence the drag coefficient for the Beagle 2 mission, will only be discussed.

Effects of Dynamic Pressure

Perhaps one of the most primary external influences affecting a canopy's drag coefficient in quasi-steady state conditions is dynamic pressure. As stated previously, since the parachute's canopy is essentially an elastic shell, the influences of dynamic pressure to transmit tension and stress throughout the canopy structure and thus influence the canopy shape and aerodynamic performance highly correlates the drag coefficient as a strong function of dynamic pressure. Since the decelerator system is generally a passive flight system (i.e., unpowered), this correlation of drag coefficient to dynamic pressure interchangeably relates to the weight of the suspended payload or the gross weight of the decelerator system in steady-state descent.

In simplified form this can be expressed as:

$$W = \left(C_D S\right)_0 Q \qquad \text{Eqt. (7)}$$

where,

W = Gross system weight

Q = Dynamic pressure

From equation (7), the following relation can be drawn:

$$W/S_0 \propto Q \propto C_{D0} \qquad \text{Eqt. (8)}$$

where,

W/S_0 = Unit canopy loading

As a result of equations (7) and (8), the influence of dynamic pressure on drag coefficient is usually expressed as a function of unit canopy loading, rate of descent under a constant altitude condition, or more directly as a function of dynamic pressure itself. Figures 5, 6, and 7 present the influence of dynamic pressure on drag coefficient for various Ringsail parachute configurations.

As stated previously, dynamic pressure directly acts upon the elastic characteristics of the canopy structure, thus influencing the canopy's drag coefficient. This

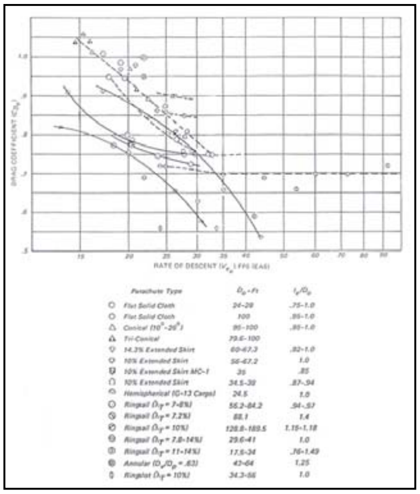

Figure 5

interaction between dynamic pressure and the canopy's elastic properties implies certain limitations of the extent by which dynamic pressure can alter canopy

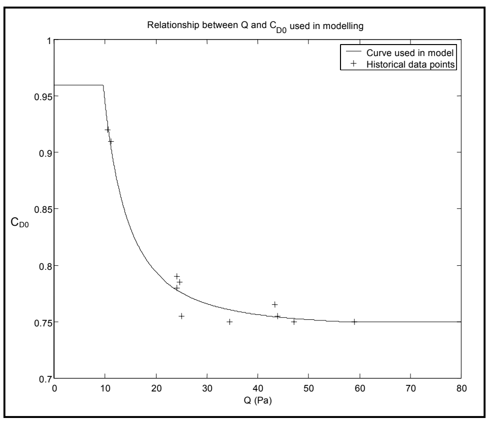

Figure 6

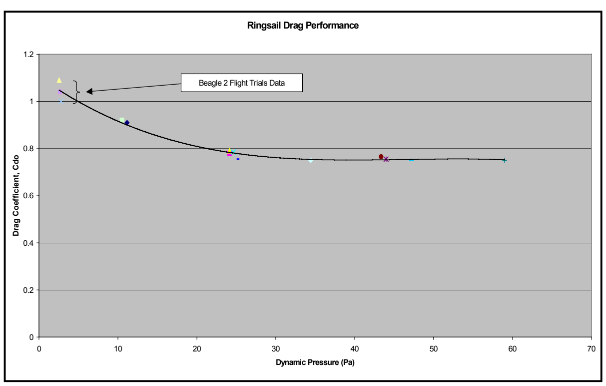

Figure 7

shape and thus the drag coefficient. Namely, for increasing dynamic pressure on a fully inflated canopy, there will be a structural limit that when reached, the canopy's elastic (and associated geometric) properties will not allow any significant changes in the canopy shape that would influence canopy drag. Hence once this limit is reached, for ever increasing dynamic pressure, the drag coefficient will remain constant (exclusive of Mach effects and inflation stability concerns). Conversely, the same can be stated of ever decreasing dynamic pressure as well.

Given that the Beagle 2 main parachute unit canopy loading is much lighter than that shown on record, full-scale flight trials of the Beagle 2 main parachute were conducted to determine the relationship between dynamic pressure and drag coefficient under the unit canopy loading conditions to be experienced during Martian descent. An estimate of the upper limit drag coefficient along with a derived function of drag coefficient versus dynamic pressure used in the preliminary modeling is provided in Figure 6. Figure 7 incorporates the results of the Beagle 2 full-scale flight trials along with other Ringsail parachute designs.

Effects of Atmosphere

In most parachute flight applications, the Reynolds numbers are very high and, as a result, viscous effects can be ignored. However, with regards to the Martian atmosphere, Reynolds numbers are very low—to the point of marginal continuum flow.

Analysis has shown that changes in the gross flow characteristics around the parachute are minimal due to Reynolds number effects as a result of the sharp edge separation that occurs due to the bluff aerodynamic nature of the parachute[ix]. However, viscous effects on the airflow through the canopy fabric (i.e., fabric permeability, λ_m) have been shown to be substantial—drastically reducing fabric permeability and in turn, the canopy total porosity. To see why this is so, Lingard suggested the following[x]:

The effective porosity of canopy fabric can be simply defined as[xi]:

$$c_e = \frac{u_0}{U} \qquad \text{Eqt. (10)}$$

where,

u_0 = Velocity through the canopy fabric

$\Delta p = \frac{1}{2}\rho U^2$ = pressure loss + viscous loss

Payne[xii] noted that:

$$\Delta p = K_1 \rho u_0^2 + K_2 \mu u_0$$

Solving for u_0:

$$u_0 = -\frac{K_2 \mu}{2K_1 \rho} + \sqrt{\frac{K_2^2}{4K_1^2 \rho^2} + \frac{\Delta p}{K_1 \rho}} \qquad \text{Eqt. (11)}$$

Combining equations (10) and (11) and solving for c_e yields:

$$c_e = -\frac{K_2}{2K_1 R_e} + \sqrt{\frac{K_2^2}{4K_1^2 R_e^2} + \frac{1}{2K_1}} \qquad \text{Eqt. (12)}$$

where,

K_1 = Constant

K_2 = Constant

$R_e = \dfrac{\rho U}{\mu}$ = Reynolds number per unit length

From equation (12), it can be shown that for decreasing Reynolds numbers, the effective porosity, c_e, also decreases. This decrease in the effective porosity reduces the overall total porosity of the canopy and, in turn, increases the canopy's drag efficiency (i.e., increased drag coefficient).

Figure 8 provides a plot of laboratory results conducted on the *Mars Pathfinder* program, which emulates Δp across the canopy fabric under Martian flight conditions (including major atmospheric constituents)[xiii]. As shown, equation (12) (i.e., the dashed-line), whose constants K_1 and K_2 were determined based upon these laboratory results, correlates reasonably well with the experimental results.

From Figure 8, the fabric porosity of the Beagle 2 main parachute for Martian flight conditions will be extremely low bringing the total porosity of the main parachute to equal essentially that of the canopy's geometric porosity. In turn, this decrease in porosity will increase the main parachute drag coefficient. For this reason, full-scale flight trials of the Beagle 2 main parachute used non-porous fabric to emulate the Reynolds number effects of the Martian atmosphere.

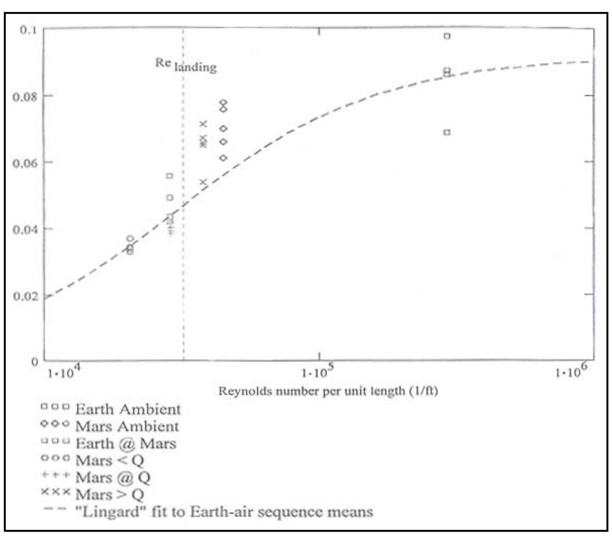

Figure 8

Aerodynamic Stability

As stated in *System Aerodynamics*, the aerodynamic interactions between the suspended payload and the parachute form a complex aerodynamic flow pattern, which in turn establishes the aerodynamic performance of the overall system. Thus, decelerator system aerodynamic stability is also borne of this same phenomenon. For example, a stable winged craft may be destabilized by the application of a drag force of a stable parachute at a point on the craft unsuitable for continued stable flight. Or, a stable parachute may be destabilized by the wake of the suspended payload. And finally, a suspended payload and parachute that are both unstable separately may be stabilized by joining them together through a suitable harness design[xiv].

The motion of a decelerator system moving freely in flight may exhibit two general classes of stability:

- *Static stability* is the tendency of a decelerator system to develop steady-state restoring moments when disturbed from a position of equilibrium.
- *Dynamic stability* is the tendency of a moving decelerator system to develop moments that act to damp unsteady motion[xv].

For brevity's sake, the focus of this discussion is on those parameters that most influence the Beagle 2 mission objectives.

Relation of Drag Coefficient to Static Stability

In large part, those influences and attributes that affect drag coefficient also affect the canopy's static stability. Namely, those drag coefficient parameters related to the canopy's inflated profile, as well as total porosity and porosity distribution, have direct bearing on the canopy's static stability performance. As such, for ballistic canopies (i.e.,

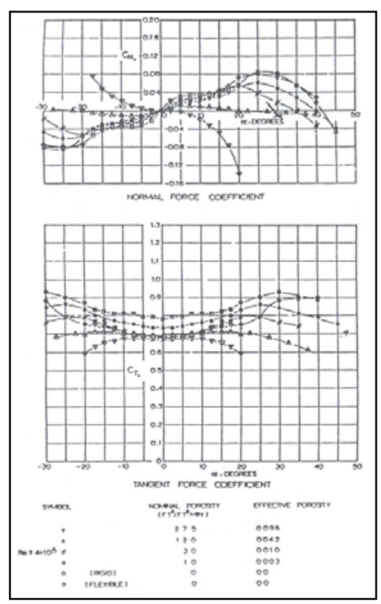

Figure 9

Ringsail, etc.), a general correlation between drag coefficient and static stability can be drawn.

As shown in Figures 9 and 10, as the canopy's total porosity decreases, the drag coefficient (or rather the canopy's resultant force vector, F_R) increases; however, the canopy's static stability decreases (i.e., equilibrium positions for $-dC_M/d\alpha$ move towards increasing α). The converse of this phenomenon is equally valid as well (i.e., increasing total porosity decreases drag coefficient and increases static stability). In like manner, with exception to scale, the attributes and influences that affect the canopy's inflated profile as relates to drag coefficient (i.e., dynamic pressure, effective line length, and planform shape) also tend to affect the canopy's static stability, i.e., *as a canopy's drag coefficient increases, its static stability decreases*. The converse of this relationship of drag coefficient to static stability is also equally valid.

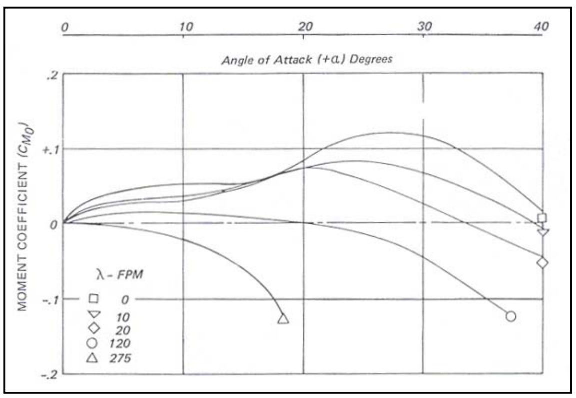

Figure 10

Figure 11 presents the effects of unit canopy loading and effective line length on system static stability as determined during full-scale flight trials on the *Viking* program.

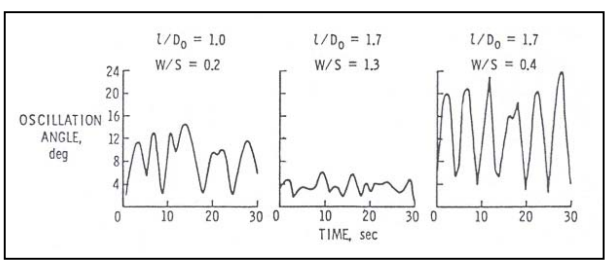

Figure 11

The relationship of drag coefficient to static stability is fundamental in the design of ballistic canopies and will predominate in the design and development of the Beagle 2 main parachute. For this reason, full-scale flights trials of the Beagle 2 main parachute measured oscillation amplitudes and, where possible, frequency of oscillations under flight conditions emulating a limited Martian environment. From these results, static stability and limited dynamic stability characteristics of the Beagle 2 main parachute were constructed. Based on analysis of the available video record, maximum oscillatory amplitudes of the Beagle 2 main parachute system were estimated to be ±12°. The system period, based on analysis of the available inclinometer data and video record, was estimated to be 15.7 seconds/cycle. Figures 12 and 13 show sample analysis results of the maximum oscillatory amplitude and period estimates from the Beagle 2 full-scale flight trials.

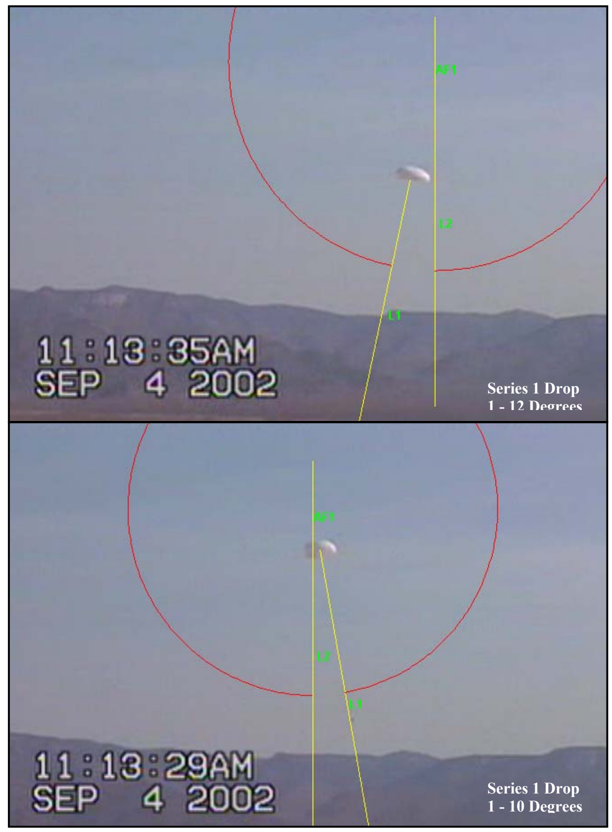

Figure 12

Relation of System Length to Dynamic Stability

Though the Beagle 2 canopy static stability is expected to behave in the manner described above, the Beagle 2 *decelerator system* dynamic stability is expected to behave in a manner uniquely of its own. The reason for this is that, unlike most other decelerator systems, the Beagle 2 system length is extremely long (~4.1 D_0). The reason offered for the system length was to abate the concern of the main parachute coming to rest over the spacecraft once the decelerator system had landed. Nonetheless, this characteristic system length also has bearing on the system flight dynamic stability.

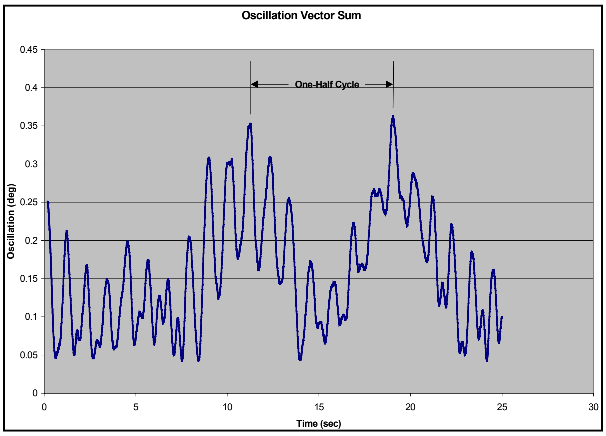

Figure 13

Gionfriddo[xvi] showed that the natural period, T_n, of a parachute-cargo system can be simplified to the following form:

$$T_n = 2\pi\sqrt{\varepsilon L} \qquad \text{Eqt. (22)}$$

where

ε = Ratio of cargo mass to that of the sum of the cargo mass and included air mass related to the cargo.

L = Non-dimensional length of line joining the centers of gravity of parachute and cargo.

Here, Gionfriddo was developing approaches to analyze the performance differences in flight dynamic stability between various parachute-cargo systems.

As shown in equation (22), it is easy to see the influence that system length has on the flight dynamic stability of decelerator systems. In fact, equation (22) explains, in large part, the large system period observed during the Beagle 2 full-scale flight trials (i.e., 15.7 seconds/cycle) as a result of the extensive system length (~4.1 D_0).

To better understand this phenomena, closer examination reveals that equation (22) correlates very well to that of the natural period of a pendulum, τ. Namely,

$$\tau = 2\pi\sqrt{\frac{l}{g}} \qquad \text{Eqt. (23)}$$

where

l = System length

g = Gravity constant

As Gionfriddo was analyzing the *performance differences* of *Earth-bound* systems, the gravity term in equation (22) is properly excluded. However, for Beagle 2, where gravity differences between Earth and Mars are significant, gravity effects cannot be excluded, wherein incorporating the assumptions of Gionfriddo[xvii] into equation (23) may be more appropriate.

Concluding, from equation (23) it is estimated that the natural period of the Beagle 2 decelerator system may increase by as much as 60% due to gravity effects alone. However, given that the maximum system oscillatory amplitude will not exceed that imposed by the flight dynamics of the main parachute (i.e., ±12°), the increased natural period will tend to further reduce the system lateral velocities due to oscillations and, thereby, prove beneficial to the functional operation of the landing airbags.

Designing the Main Parachute

The basic design goal driving the definition of the Beagle 2 main parachute was to maximize the drag area per pound of weight. The volume available for the Main Parachute was ample from the outset. This presented a challenge to design the largest, drag-efficient, parachute within the constraints of the loads environment and mass budget. In order to achieve this goal, a departure from the standard Disc-Gap-Band type parachute was deemed necessary. A Ringsail parachute was selected for this mission due to the designs exceptional drag efficiency and historical performance in a plethora of both high-altitude and man-rated earth landing applications.

Determination of Canopy Size

The rate of descent requirement for surface impact was specified as 18 m/s maximum with a design goal of 16 m/s. Since the dynamic pressure at terminal descent is lighter than that on historical record, the actual drag coefficient was expected to be higher. Also, other contributing factors were thought to add to a higher drag coefficient as well (i.e., porosity, etc.). The concern with a very high drag coefficient is its effects on static stability. Therefore, the design approach taken was to assume a nominal, albeit conservatively lower, drag coefficient, similar to that on the historical record wherein the static stability was deemed reasonable (i.e., approx. ± 10°) and size the canopy based upon this lower nominal drag coefficient. It was accepted that a drag-coefficient of 0.92 was certainly achievable with a Ringsail Planform, so the designers proceeded to determine a canopy size based on the predicted loads and mass budget constraints. A number of iterations resulted in a canopy diameter determination of 10.02m (32.87ft).

Determination of Canopy Porosity

Based upon full scale Ringsail design data, the geometric crown porosity selected for the Beagle 2 main parachute was 2.4%. This was primarily based on the Mercury Ringsail design parameters that provided excellent inflation stability. The following design parameters were also incorporated into the canopy:

- The vent area is as small as possible (i.e., $S_V \leq 0.5\% \; S_0$)
- Minimum of approximately two inches between radial seam centerlines at vent.

Once the above dimensions were established, the basic gore outer boundaries were determined. From here, the individual gore is divided up into a number of panels. The panels themselves are trapezoidal in shape wherein the widths of the panel leading edge (i.e., that side closest to the skirt) and trailing edge (i.e., that side closest to the vent) match the gore width at the appropriate radial gore height (excluding panel fullness discussed later). Thus, one can view the gore shape as being approximated by a number of trapezoidal panels.

The ringslot section comprises approximately 30% to 40% of the gore height as measured from the vent[xviii]. The primary objective in the gore design of the ringslot section is to ensure that the appropriate amount of geometric crown porosity, λ_{gc}, is incorporated into the gore. The general guidelines recommended for this objective are:

- The geometric crown porosity contribution of the slots (i.e., radial spaces) should be equally distributed over approximately 30% to 40% of the gore height as measured from the vent.
- The maximum slot width should not exceed four inches.
- The geometric crown porosity is *inclusive* of the vent area.

As a result of the guidelines above, it is not uncommon for the individual ringslot panel heights to vary (i.e., the distance on the panel that traverses along the gore height) or significantly vary in height from the ringsail patterns.

With the ringslot section completed in the manner above, the design of the ringsail section of the gore is simply approached as making the number of remaining panels in the gore (i.e., N_p less the number of ringslot panels, N_{slot}) all the same panel height. As with the ringslot panels, the trailing edges of the ringsail panels have no fullness and thus, equal the gore width at the appropriate radial gore height. The leading edges of the ringsail panels; however, incorporate fullness. This fullness, which gives the Ringsail parachute its name, provides a number of benefits.

In the early inflation phase, inflow from not only the mouth inlet but also the leading edge of each ringsail panel takes place, thus contributing to more reliable, albeit faster, parachute inflation. Also during steady-state descent, the crescent slots of the ringsail panels act as aerodynamic strakes in limiting the shed vortices and leading to good stability.

However, as the leading edge fullness increases, the leading edge to trailing edge load sharing potential decreases. Thus, a practical limit on leading edge fullness is reached around 10% to 12%[xix].

The leading edge fullness of the ringsail panels can vary from 0% to 12% and is typically distributed in variation from least fullness (located on the ringsail pattern closest to the vent) to the most fullness (located on the ringsail panel at the skirt). As imaginable, this distribution can, and has, taken on various forms and combinations. There is no standard guideline on how the ringsail leading edge fullness should be distributed along the radial gore height other than the recommendation that the canopy's overall average panel fullness should be approximately 4%[xx]. For the Beagle 2 main parachute, the leading edge sail fullness distribution is the same as that used on recent successful Ringsail parachute programs whose distribution varies from 0% to 12%.

Regarding the lead panel fullness (i.e., the ringsail panel whose leading edge is the canopy skirt), Ewing's original concept was to set the lead panel edge fullness to zero. Delurgio[xxi] summarizes this design concept as being best described as an Extended Skirt effect that would allow the best possible stability by providing ideal tangent flow at the skirt plane. This leading panel design concept was also successfully applied to recent Ringsail parachute programs yielding excellent stability results. Based upon the success of these programs, zero leading edge fullness in the lead panel was incorporated into the Beagle 2 main parachute.

Determination of Final Canopy Planform

The gore design is by necessity an iterative process. The canopy Planform was determined using a 3-dimensional surface model. A quarter-spherical shaped surface was defined with an area equal to that of the nominal surface area, S_0. From this quarter-sphere, the radial height and general width dimensions of the individual panels were determined. The theoretical 3-dimensional locations of the panel nodes were then described in the model (See Figure 14).

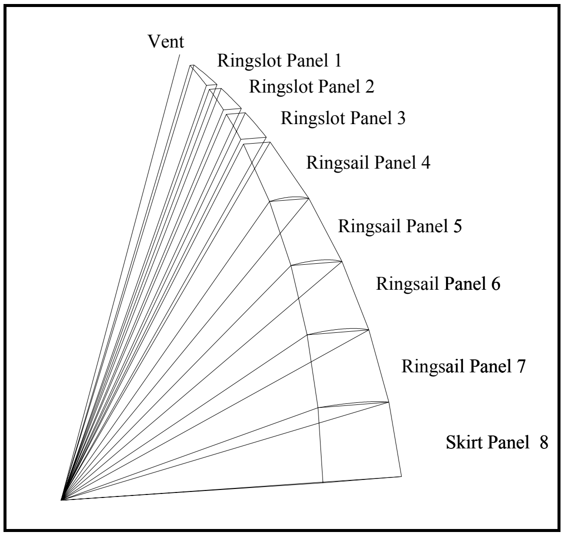

Figure 14

The number of gores was selected based on load predictions and material availability. The gore count was established at 28, which was then built into the parachute model to establish the full fidelity Planform definition. The final definition of the surface model is illustrated in Figure 15 below.

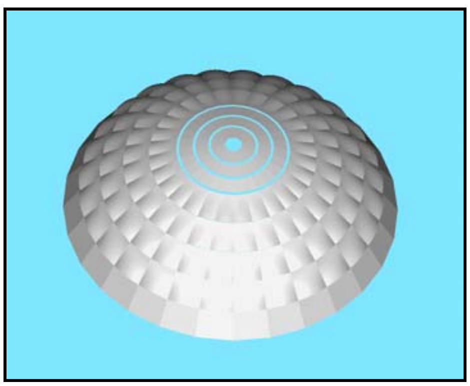

Figure 15

Figure 16 summarize the basic dimensions of the general gore layout of the Beagle 2 main parachute. Figure 17shows the approximate inflated shape.

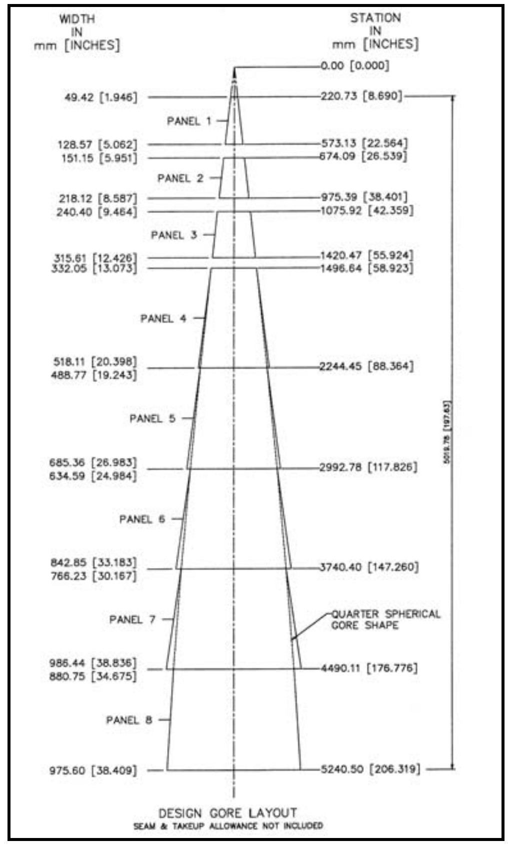

Figure 16

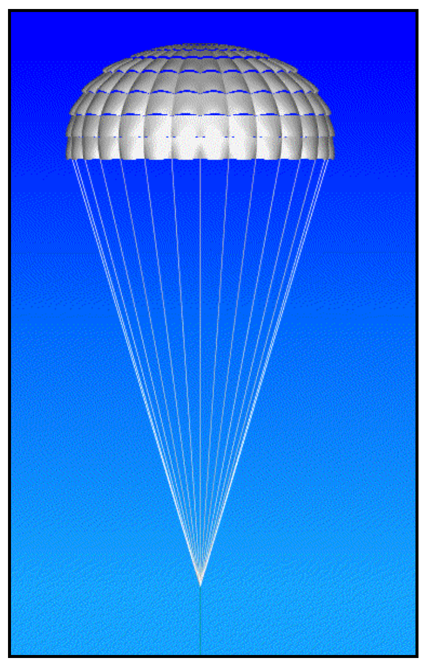

Figure 17

Miscellaneous Design Features

The suspension line length was established from historical data on ringsail performance, primarily based on the Irvin Aerospace Inc 156 ft diameter, which employed a line length ratio (L_s/D_o) of 1.15. This ratio was incorporated into the Beagle 2 Main Parachute also. The canopy also incorporated pocket bands located at every gore. The canopy employed a sacrifice panel for abrasion protection during deployment and for inflation control.

Manufacturing Challenges

From the outset, the design team set a goal of building one of the most efficient canopies in terms of drag-area per pound that had ever been attempted. This involved the use of super lightweight materials and construction methods. The suspension lines and radials were manufactured from 100 lb tensile Spectra® cord and the canopy was fully rigged with this material. In addition to this, extremely lightweight canopy broadcloth was developed to make the drag-producing surface of the canopy. This cloth was approximately 20% lighter than MIL-C-7020 type 1 and weighed in at 0.8 oz/yd^2. The combination of these materials led to a very difficult construction but techniques were developed to ensure that the main seams were of consistently high quality. Figure 18 shows an example of the main seam configuration.

Figure 18

Main Parachute Testing

Following the design of the Main Parachute, a very aggressive test campaign was developed to verify the performance. Initially 3 test series were engaged to test the following.

Test Series 1

This test series was intended to quantify the following performance parameters:

- Inflation Profile
- Drag Area
- Stability

These tests were conducted at Redlake, AZ. This location is a dry lakebed close to Kingman, AZ. The test aircraft was a C-123 Provider.

The Drop-Zone (DZ) at Redlake is ideally suited to this type of parachute testing. It is extremely large and is totally free from ground obstacles. This type of terrain is essential to ensure that no ground damage occurs to the test articles. The DZ is 2800 ft Above Mean Sea Level (AMSL).

The weather conditions required that all tests were conducted, early morning (dawn) or early evening (dusk) the temperatures during the day rose to a level that is not conducive to good-quality data acquisition due to the atmospheric perturbations arising from thermal activity.

The test articles were all zero porosity versions of the flight version to duplicate the low density environment that would be experienced during the mission.

The test vehicle for series 1 testing was designed to provide the following physical properties:

Nomenclature	Values (SI)	Values (Imperial)
Weight	182.8 N	41.1 lbs
MOI (I_{xx}, I_{yy}, I_{zz})	0.647, 0.668, 1.051 kg-m^2	0.477, 0.493, 0.775 slug-ft^2
Distance from CG to Main parachute attachment	71 mm	2.8 inch

Figures 19, 20, and illustrates the general layout of the test vehicle.

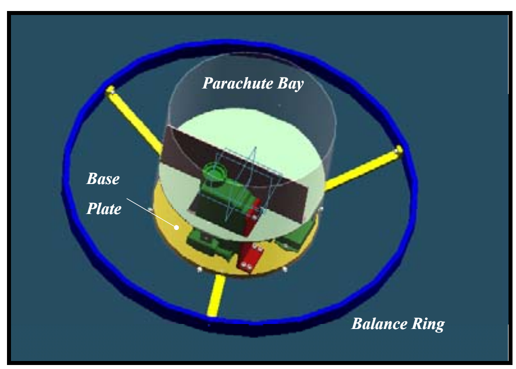

Figure 19

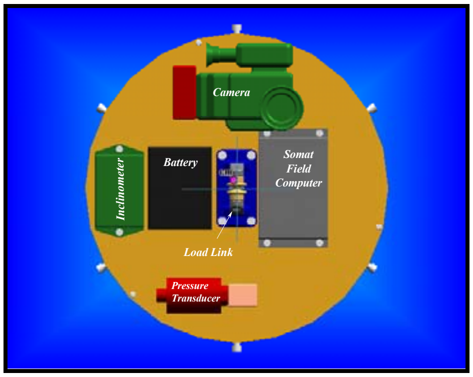

Figure 20

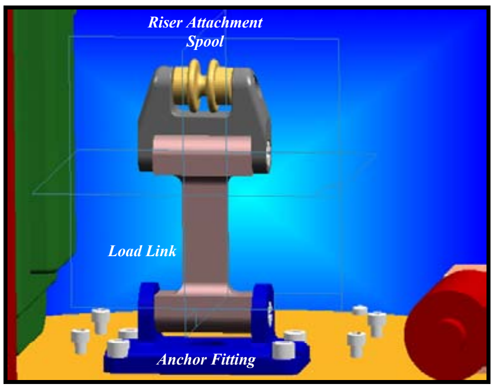

Figure 21

Test Series 2

This test series was intended to examine and quantify the following performance parameters:

- Inflation Profile
- Structural Integrity

These tests were conducted at Apple Valley, CA. and used the same test vehicle as series 1, but incorporated additional ballast to increase the opening forces. It was hoped that limit load conditions could be achieved during this series. An illustration of the test vehicle is shown in Figure 22 below.

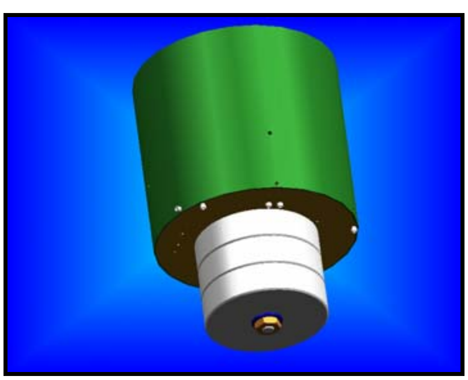

Figure 22

Test Series 3

This test series was established to ensure that the deployment system would function satisfactorily at the high strip out velocities.

Test Instrumentation

Each of the drop test vehicles were instrumented with the following sensors.

- Load Link
  1000Hz
  (Riser Tension)
- Pitch Plane Inclinometer
  500 Hz
  (X-Axis Oscillation)
- Yaw Plane Inclinometer
  500 Hz
  (Y-Axis Oscillation)
- Static Pressure
  100 Hz
  (Air Pressure)
- Thermocouple
  100 Hz
  (Air Temperature)

In addition to the on-board instrumentation, 3 cameras were employed for subsequent film analysis of each test, 2 ground cameras and 1 on-board camera. The ground cameras were positioned perpendicular to each other (see Figure 23) to enable subsequent stability analysis.

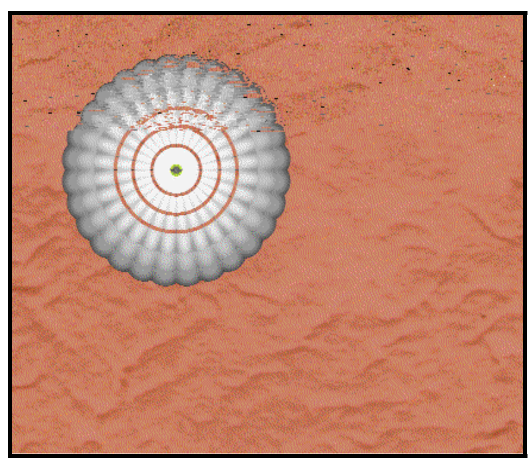

Figure 23

Test Results

All of the tests confirmed the performance of the Beagle 2 Ringsail Main parachute exceeded the requirements. During test series 2 it became apparent that we could get close to the loading conditions required for a limit load test but could not match both loads and dynamic pressure simultaneously. This led to a potential overload condition of the drag surface. In order to ensure the structural integrity of the entire system a test methodology had to be determined very quickly to keep the program on schedule. Budget and time constraints did not give us the option of a wind tunnel series or a high-altitude balloon test. To this end a simple tow-test was designed to impart the maximum dynamic pressure on the full open canopy. The canopy was inflated behind a truck and towed across the Redlake Dry Lake Bed. Velocity, Parachute Load and Air Density were monitored to ensure the proof load conditions were met and the parachute performed flawlessly. The canopy consistently demonstrated a drag-coefficient approaching unity and stability of better than ± 8°, some departures out to 12° were observed during the tests, but these tended to be random events caused by atmospheric perturbations. The canopy quickly recovered from these disturbances. Figure 24 shows the canopy during a drop test and Figure 25 shows the canopy during the Tow Test.

Figure 24

Figure 25

Acknowledgements

The authors gratefully acknowledge the contributions of all the team members to the work presented herein as well as the permission of Astrium, Ltd, England to publish this paper. A special thanks is also acknowledged to Mr. Jim Blumenthal, the owner and operator of the C-123 aircraft and flight test facilities, as well as Mr. John McNish for their helpful contributions towards flight test operations. Finally, special thanks are offered to Messrs: Alan Haigh (Astrium) and Dave Northey (Analyticon) who led the development teams and made an extremely challenging program personally rewarding and fun.

References

[i] Fallon II, Edward J.; *System Design Overview of the Mars Pathfinder Parachute Decelerator Subsystem*; AIAA paper no. 97-1511; 14th AIAA Aerodynamic Decelerator Systems Technology Conference; June 1997.

[ii] Steinberg, S., Siemers, P., and Slayman, R.; *Development of the Viking Parachute Configuration by Wind Tunnel Investigation*; AIAA 4th Aerodynamic Deceleration Systems Conference; AIAA paper no. 73-454; Palm Springs, CA; 21-23 May 1973.

[iii] Corridan, R., Givens, J., and Kepley, B.; *Transonic Wind Tunnel Investigation of the Galileo Probe Parachute Configuration*; AIAA 8th Aerodynamic Decelerator and Balloon Technology Conference; AIAA paper no. 84-0823; Hyannis, MA; 2-4 April

1984.

[iv] Lingard, J. and Underwood, J.; *Wind Tunnel Testing of Disk-Gap-Band Parachutes Related to the Cassini-Huygens Mission*; RaeS/AIAA 12th Aerodynamic Decelerator Systems Technology Conference and Seminar; AIAA paper no. 98-1200; London, UK; 10-13 May 1993.

[v] Campbell, J.F. and Brown Jr., C.A.; *Evaluation of Experimental Flow Properties in the Wake of a Viking '75 Entry Vehicle*; AIAA paper no. 73-475; AIAA 4th Aerodynamic Deceleration Systems Conference; Pal Springs, CA; May 1973.

[vi] Preisser, J.C. and Greene, G.C.; *Effect of Suspension Line Elasticity on Parachute Loads*; Journal of Spacecraft and Rockets, vol. 7 no. 10, pp. 1278-1280; October 1970.

[vii] Jacobsen, L.S. and Ayre, R.S.; Engineering Vibrations, Chap. 4; McGraw-Hill; New York; 1958.

[viii] Ewing, E.G., Bixby, H.W., and Knacke, T.W.; Recovery Systems Design Guide; AFFDL-TR-78-151; Air Force Flight Dynamics Laboratory, Wright-Patterson Air Force Base, Ohio; June 1978; pp. 336-337.

[ix] Lingard, J.S., Underwood, J.C.; *The Effects of Low Density Atmosphere on the Aerodynamic Coefficients of Parachutes*; 13th Aerodynamic Decelerator Systems Technology Conference; AIAA paper no. 95-1556; May 1995.

[x] Ibid.

[xi] Heinrich, H.G. and Haak, E.L.; Stability and Drag of Parachutes with Varying Effective Porosity; ASD-TDR-62-100; Aeronautical Systems Division; Wright-Patterson AFB; September 1962.

[xii] Payne, P.R.; *The Theory of Parachute Fabric Porosity as Applied to Parachutes in Incompressible Flow*; The Aeronautical Quarterly, vol. 29; August 1978.

[xiii] Fallon II, Edward J.; *System Design Overview of the Mars Pathfinder Parachute Decelerator Subsystem*; AIAA paper no. 97-1511; 14th AIAA Aerodynamic Decelerator Systems Technology Conference; June 1997.

[xiv] Ewing, E.G., Bixby, H.W., and Knacke, T.W.; Recovery Systems Design Guide; AFFDL-TR-78-151; Air Force Flight Dynamics Laboratory, Wright-Patterson Air Force Base, Ohio; June 1978; pp. 299.

[xv] Ibid.

[xvi] Gionfrido, Maurice Paul.; *A Method for Determining Airdrop System Characteristics for Minimum Altitude Loss to Equilibrium*; Master Thesis; Massachusetts Institute of Technology; January, 1969.

[xvii] Ibid.

[xviii] Delurgio, P.R. and North, R.N.; *Parametric Analysis and Design Considerations for Mars Parachute Landing System*; TP 121; AIAA Aerodynamic Deceleration Systems Conference; Houston, TX; September 1966.

[xix] Ibid.

[xx] Ewing, E.G.; *Technical Justification for Two Advanced Design Principles Recommended for Ringsail Parachutes*; Memo; 1971.

[xxi] Delurgio, Phillip R.; *Evolution of the Ringsail Parachute*; AIAA paper no. 99-1700; 15th CEAS/AIAA Aerodynamic Decelerator Systems Technology Conference; June 1999.